WHY OPTICAL AND MECHANICAL GYROS MEASURE THE SAME ANGULAR RATE RELATIVE TO NON-ROTATING INERTIAL SPACE

Paul G. Savage
Strapdown Associates, Inc.
Maple Plain, MN 55359 USA

WBN-14031
www.strapdowassociates.com
December 21, 2022

ABSTRACT

A question has arisen in some inertial engineering circles as to why optical gyros (based on Einstein's constant-speed-of-light Relativity principle) measure the same angular rate as mechanical gyros (based on Newton's dynamic law of mass response to applied force). This article shows that the answer stems from both gyro types being based on the same fundamental Coriolis kinematic rotation equation relating vector component measurements in coordinate frames at rotation relative to one-another. The Relativity laws of Einstein and Dynamics laws of Newton are valid in inertially non-rotating coordinates, not in coordinates affixed to a rotating gyro where the gyro readout mechanism is located. Using the Coriolis rotation equation for gyro implementation (based either on Relativity or Newtonian Dynamics) provides the means for translating these laws from non-rotating inertial space (in which they are valid) into rotating gyro coordinate output axes. Beginning with the fundamental Coriolis kinematic rotation equation, this article analytically derives the input/output expressions for optical ring laser gyros, optical fiber optic gyros, mechanical MEMS (Micro-machined Electro-Mechanical System) gyros, and for mechanical spinning rotor gyros, demonstrating that each measures angular rotation relative to non-rotating inertial space.

NOTATION

$\underline{V}$ = Vector without specific coordinate frame designation. A vector is a parameter that has length and direction. Vectors used in the paper are classified as "free vectors", hence, have no preferred location in coordinate frames in which they are analytically described.

$\underline{V}^A$ = Column matrix with elements equal to the projection of $\underline{V}$ on Coordinate Frame A axes. The projection of $\underline{V}$ on each Frame A axis equals the dot product of $\underline{V}$ with the coordinate Frame A axis unit vector.

$\left(\underline{V}^A\times\right)$ = Skew symmetric (or cross-product) form of $\underline{V}^A$ represented by the square

matrix $\begin{bmatrix} 0 & -V_{ZA} & V_{YA} \\ V_{ZA} & 0 & -V_{XA} \\ -V_{YA} & V_{XA} & 0 \end{bmatrix}$ in which V_{XA}, V_{YA}, V_{ZA} are the components of $\underline{V}^A$. The matrix product of $\left(\underline{V}^A\times\right)$ with another *A* Frame vector equals the cross-product of $\left(\underline{V}^A\times\right)$ with the vector in the *A* Frame, i.e., $\left(\underline{V}^A\times\right)\underline{W}^A = \underline{V}^A\times\underline{W}^A$.

C_{A1}^{A2} = Direction cosine matrix that transforms a vector from its Coordinate Frame A_2 projection form to its Coordinate Frame A_1 projection form.

$\underline{\omega}_{A_1A_2}$ = Angular rate of Coordinate Frame A_2 relative to Coordinate Frame A_1. When A_1 is non-rotating, $\underline{\omega}_{A_1A_2}$ is the angular rate that would be measured by angular rate sensors mounted on Frame A_2.

INTRODUCTION

Both optical and mechanical gyros measure angular rotation relative to non-rotating inertial space. Optical gyros are based on Einstein's Theory of Relativity while mechanical gyros are based on Newton's laws of dynamics. Based on such different theories, why do optical and mechanical gyros measure the same angular rotation? The elusive answer is surprising simple: Because both gyro types are based on the same kinematic relation (Eq. (A-10) derived in Appendix A), relating the differential change in a vector's components as projected onto non-rotating and rotating coordinate frames:

$$d\underline{\xi} = d\underline{\Xi} + d\underline{\Psi}\times\underline{\xi} \qquad (1)$$

where $d\underline{\Psi}$ is a differential angular rotation of the rotating frame relative to non-rotating inertial space, $\underline{\xi}$ is an arbitrary vector, $d\underline{\xi}$ is the differential change in vector $\underline{\xi}$ as measured in the non-rotating frame during the $d\underline{\Psi}$ rotation, and $d\underline{\Xi}$ is the equivalent to $d\underline{\xi}$ that would be measured in the rotating frame during the $d\underline{\Psi}$ rotation. Eq. (1) is the basis for the design of optical ring laser gyros (RLGs), optical fiber optic gyros (FOGs), MEMS (Micro-machined Electro-Mechanical Systems) mechanical gyros, and spinning rotor mechanical gyros. The equivalency of (1) to each gyro type is described next.

For an optical gyro (RLG or FOG), $d\underline{\Psi}$ in (1) represents a differential angular rotation of the gyro relative to non-rotating inertial space (and the angular increment being sensed). Two vectors within the gyro are each represented by $\underline{\xi}$ in (1), each from a fixed point to a photon within a gyro generated mono-chromatic light wave. The photons travel in opposite directions, both within a closed waveguide built into the gyro. The $d\underline{\xi}$, $d\underline{\Xi}$ parameters in (1) represent

differential changes in $\underline{\xi}$ for the counter-travelling photons that would be measured in non-rotating space ($d\underline{\xi}$) and in the rotating gyro ($d\underline{\Xi}$). Angular rotation induces a Doppler-like shift in the light beam wavelengths, positive for the beam travelling in the direction of rotation, negative for the beam travelling opposite to the opposite. From Einstein's law of Special Relativity, the velocity of each light wave will be the same (speed of light), thereby transforming the wavelength shift into a corresponding frequency shift between the counter-travelling waves. Readout detectors built into the gyro sense the frequency difference between the counter-travelling waves, converting it into the angular rotation that produced it.

For a common MEMS type mechanical gyro, $d\underline{\Psi}$ in (1) represents a differential angular rotation of the gyro relative to non-rotating inertial space (and the angular increment being sensed); $\underline{\xi}$ in (1) represents the distance vector in the gyro between two separate linearly vibrating masses micro-machined into the MEMS silicon substrate, and $d\underline{\xi}$, $d\underline{\Xi}$ in (1) represent differential changes in $\underline{\xi}$ that would be measured in non-rotating space ($d\underline{\xi}$) and in the rotating gyro ($d\underline{\Xi}$) during the $d\underline{\Psi}$ rotation. Angular rotation produces Coriolis accelerations (changes within $d\underline{\xi}$, $d\underline{\Xi}$) which, through Newton's laws of dynamic motion, generate reaction forces measured by sensors (accelerometers) micro-machined into the vibrating masses. Subtracting the accelerometer outputs eliminates their response to linear acceleration, leaving an angular rotation induced measurement for output.

For a spinning rotor type mechanical gyro, $d\underline{\Psi}$ in (1) represents an infinitesimally small angular rotation relative to non-rotating inertial space of a housing containing the gyro rotor, $\underline{\xi}$ in (1) represents an angular momentum vector generated by the composite motion of all mass points within the gyro housing, and $d\underline{\xi}$, $d\underline{\Xi}$ in (1) represent differential changes in the angular momentum vector during the $d\underline{\Psi}$ rotation as measured in non-rotating coordinates ($d\underline{\xi}$) and in coordinates that rotate with the gyro housing ($d\underline{\Xi}$).

This article analytically shows how Eq. (1) leads to the input/output relationship for each of these gyro types.

OPTICAL GYROS

Optical gyros contain a closed-optical path containing two overlapping beams of monochromatic light (a "*p*" wave and a "*q*") traveling in opposite directions [1], [2]. Optical gyros implement four versions of (1): two for the *p* wave and two for the *q* wave. For the *p* wave, the two versions of $\underline{\xi}$ are denoted as $\underline{x}_{p/i}$ and $\underline{x}_{p/a}$ where *a* and *i* are fixed points within the rotating body (point *i* located within the *p* beam wave-path), *p* designates a photon travelling with the *p* beam, $\underline{x}_{p/i}$ is the linear distance vector from point *i* to photon *p*, and $\underline{x}_{p/a}$ is the linear distance vector from point *a* to photon *p*. For the change in $\underline{\xi}$ relative to non-rotating space ($\Delta\underline{\xi}$), the analogous inertial frame changes in $\underline{x}_{p/i}$, $\underline{x}_{p/a}$ are $\Delta\underline{x}_{p/i}$, $\Delta\underline{x}_{p/a}$.

For the change in $\underline{\xi}$ relative to rotating space (i.e., $d\underline{\Xi}$) we define $\Delta\underline{\chi}_{p/i}$, $\Delta\underline{\chi}_{p/a}$ as the corresponding changes in $\underline{x}_{p/i}$, $\underline{x}_{p/i}$ relative to the rotating body. For the small angular change in rotating space $\Delta\underline{\psi}$ corresponding to the infinitesimal $d\underline{\psi}$ in (1), we define $\Delta\underline{\theta}$ as the small incremental angular rotation of the *p*, *q* optical paths during the $\Delta\underline{x}_{p/i}$, $\Delta\underline{x}_{p/a}$, $\Delta\underline{\chi}_{p/i}$, $\Delta\underline{\chi}_{p/a}$ position change time interval.

Applying (1) to the previous definitions finds

$$\Delta\underline{x}_{p/i} = \Delta\underline{\chi}_{p/i} + \Delta\underline{\theta}\times\underline{x}_{p/i} \qquad \Delta\underline{x}_{i/a} = \Delta\underline{\chi}_{i/a} + \Delta\underline{\theta}\times\underline{x}_{i/a} \tag{2}$$

Based on the definition of points *a* and *i* being fixed within the rotating body and *p* approximately overlapping *i*:

$$\underline{x}_{p/i} \approx 0 \qquad \Delta\underline{\chi}_{i/a} = 0 \tag{3}$$

Then (2) simplifies to

$$\Delta\underline{x}_{p/i} = \Delta\underline{\chi}_{p/i} \qquad \Delta\underline{x}_{i/a} = \Delta\underline{\theta}\times\underline{x}_{i/a} \tag{4}$$

We now define $\underline{x}_{p/a}$ as the distance vector from point *a* to photon *p* such that

$$\underline{x}_{p/a} = \underline{x}_{p/i} + \underline{x}_{i/a} \;\therefore\; \Delta\underline{x}_{p/a} = \Delta\underline{x}_{p/i} + \Delta\underline{x}_{i/a} \tag{5}$$

Substituting (4) in (5) obtains

$$\Delta\underline{\chi}_{p/i} = \Delta\underline{x}_{p/i} \qquad \Delta\underline{x}_{p/a} = \Delta\underline{\chi}_{p/i} + \Delta\underline{\theta}\times\underline{x}_{i/a} \tag{6}$$

Further analysis of (6) shows that

$$\frac{\left|\Delta\underline{x}_{p/a}\right|}{\left|\Delta\underline{\chi}_{p/i}\right|} = \sqrt{\frac{\Delta\underline{x}_{p/a}\cdot\Delta\underline{x}_{p/a}}{\Delta\underline{\chi}_{p/i}\cdot\Delta\underline{\chi}_{p/i}}} \approx 1 + \frac{\Delta\underline{\chi}_{p/i}\cdot\left(\Delta\underline{\theta}\times\underline{x}_{i/a}\right)}{\left|\Delta\underline{\chi}_{p/i}\right|\left|\Delta\underline{\chi}_{p/i}\right|} = 1 + \frac{\left(\underline{x}_{i/a}\times\Delta\underline{\chi}_{p/i}\right)\cdot\Delta\underline{\theta}}{\left|\Delta\underline{\chi}_{p/i}\right|^2} \tag{7}$$

For $\Delta\underline{\chi}_{p/i}$ then specialized to represent a wavelength distance $\lambda_{p/i}$ of the *p* light wave measured at point *a* on the rotating body (i.e., $\Delta\underline{\chi}_{p/i} = \lambda_{p/i}\,\underline{u}_{p/i}$ where $\underline{u}_{p/i}$ is a unit vector in the direction of the *p* wave at point *a*), [2] shows that (7) leads to

$$\frac{\left|\Delta \underline{x}_{p/a}\right|}{\left|\Delta \underline{\chi}_{p/i}\right|} = \frac{\lambda_{0_p}}{\lambda_{p/i}} = 1 + \frac{\left[\underline{x}_{i/a} \times \left(\lambda_{p/i}\, \underline{u}_{p/i}\right)\right] \cdot \Delta \underline{\theta}}{\lambda_{p/i}^2} = 1 + \left(\underline{x}_{i/a} \times \underline{u}_{p/i}\right) \cdot \frac{\Delta \underline{\theta}}{\lambda_{p/i}}$$
$$= 1 + \frac{\left(\underline{x}_{i/a} \times \underline{u}_{p/i}\right)}{V_{p/i}} \cdot \frac{\Delta \underline{\theta}}{\Delta t_{p/i}} \approx 1 + \frac{\left(\underline{x}_{i/a} \times \underline{u}_{p/i}\right)}{V_{p/i}} \cdot \frac{d\underline{\theta}}{dt_{p/i}} \qquad (8)$$

where λ_{0_p} is the p light wavelength that would be measured at point a in non-rotating inertial space, $V_{p/i}$ is the p wave velocity that would be measured at point a on the rotating body (i.e., $V_{p/i}\, \Delta t_{p/i} = \left|\Delta \underline{\chi}_{p/i}\right| = \lambda_{p/i}$), and the differential d has been substituted for the small but finite Δ change.

Thus far, the derivations leading to (8) have been based on classical Euclidean vector geometry. To continue the analysis for optical gyros, we now incorporate a basic precept of Relativity theory: that the speed of light is the same constant when measured at any point in non-rotating inertial space [3 Part 1 Chapter 11]. Hence, since $d\underline{x}_{p/i}$ is the differential distance movement of p in non-rotating space at point i, and since $d\underline{x}_{p/i}$ occurs over differential time interval $dt_{p/i}$, it follows that the speed of p over $dt_{p/i}$ will be the speed of light c, i.e., $\left|d\underline{x}_{p/i}\right| / dt_{p/i} = c$. But from (6), $d\underline{x}_{p/i} = d\underline{\chi}_{p/i}$, and therefore, $\left|d\underline{\chi}_{p/i}\right| / dt_{p/i} = c$. It follows then, that $V_{p/i} \equiv \left|d\underline{\chi}_{p/i}\right| / dt_{p/i} = c$. Thus, <u>relative to the rotating body</u>, the magnitude of the p wave velocity at point i will also be the speed of light c. This finding is the fundamental basis for optical gyros being able to measure angular rotation relative to non-rotating inertial space. For $dt_{p/i}$ redefined to be a specified differential time increment dt (<u>relative to the rotating body</u>), the finding directly links $\left|d\underline{\chi}_{p/i}\right|$ to dt. Then, with $V_{p/i} = c$ and $dt_{p/i} = dt$, (8) gives the important result:

$$\frac{1}{\lambda_{p/i}} = \frac{1}{\lambda_{0_p}} \left[1 + \frac{\left(\underline{x}_{i/a} \times \underline{u}_{p/i}\right)}{c} \cdot \frac{d\underline{\theta}}{dt}\right] \qquad (9)$$

To distinguish the opposite travel directions of the p and q waves, we designate $\underline{u}_i$ as a general wave path direction unit vector parallel to the p wave travel direction $\underline{u}_{p/i}$ at point i (i.e., $\underline{u}_i \equiv \underline{u}_{p/i}$). Thus, (9) becomes

$$\frac{1}{\lambda_{p/i}} = \frac{1}{\lambda_{0_p}}\left[1 + \frac{\left(\underline{x}_{i/a} \times \underline{u}_i\right)}{c} \cdot \frac{d\underline{\theta}}{dt}\right] \tag{10}$$

A similar derivation applies for the *q* wave. Because the *q* wave is defined to travel oppositely from the *p* wave along the same wave path, $\underline{u}_{q/j} = -\underline{u}_j$, where $\underline{u}_j$ is the direction of the *p* wave as it passes point *j* in the wave path. Then the *q* wave equivalent to (10) becomes

$$\frac{1}{\lambda_{q/j}} = \frac{1}{\lambda_{0_j}}\left[1 - \frac{\left(\underline{x}_{j/a} \times \underline{u}_j\right)}{c} \cdot \frac{d\underline{\theta}}{dt}\right] \tag{11}$$

Finally, because the *p* and *q* waves in an optical gyro emanate from the same monochromatic light source (the helium-neon plasma in a ring laser gyro or a super luminescent diode in a fiber optic gyro – described subsequently), $\lambda_{0_p} = \lambda_{0_j} = \lambda_0$, where λ_0 is the characteristic wavelength of each monochromatic light beam under zero rotation rate. Then (10) and (11) become the final forms

$$\frac{1}{\lambda_{p/i}} = \frac{1}{\lambda_0}\left[1 + \frac{\left(\underline{x}_{i/a} \times \underline{u}_i\right)}{c} \cdot \frac{d\underline{\theta}}{dt}\right] \qquad \frac{1}{\lambda_{q/j}} = \frac{1}{\lambda_0}\left[1 - \frac{\left(\underline{x}_{j/a} \times \underline{u}_j\right)}{c} \cdot \frac{d\underline{\theta}}{dt}\right] \tag{12}$$

Eqs. (12) show that the wavelength of the *p* and *q* beams will differ at points *i* or *j* along their respective wave paths in proportion to the angular rate of the gyro relative to non-rotating inertial space $d\underline{\theta} / dt$. The wavelength difference between the counter-rotating beams provides the means for measuring angular rate.

Because both light beams in an optical gyro traverse the same wave-path (in opposite directions), during each closed circuit (relative to the rotating gyro), the total distance *L* traveled around the circuit will be the same for each beam. Thus, since the oppositely directed beams travel at the same speed of light *c* through the same distance *L*, the transit time *T* around the closed-circuit will be the same: $T = L / c$. (Note: The previously stated same distance premise may not be obvious to some readers because, as is commonly known by optical gyro designers, angular rate will cause the closed circuit distance traveled by the beams to differ, but relative to non-rotating inertial space. However, if one can imagine a measuring tape graduated in both directions being attached along the closed wave-path, it should be clear that the distance measured along the tape will be the same for either measurement direction because for each, it is the same physical tape being used for the measurement.)

In the absence of rotation, (12) shows that the wavelengths of both beams will be equal, and upon completing a closed-circuit (each traveling the closed distance *L* over time interval *T*), the number of waves filling the wave-path (i.e., the total cumulative phase in wavelengths from entry to exit) will be the same. (Note: The total phase angle from peak-to-peak of a light wave can be represented as one cycle or as 2 π radians). Thus, without rotation, the cumulative phase

between the beams at exit time *T* will be the same, and the phase difference will be zero. Under rotation, however, (12) shows that the wavelength of the beam traveling with rotation will become longer (and conversely for the beam traveling in the opposite direction), hence, the cumulative phase over *L* will be less for the beam traveling with rotation. The result is that at *T*, the phase difference between the beams will differ from what it was when the closed-path journey began. The phase difference is proportional to the inertial angular rate around the gyro input axis, and is optically measured at *T* to determine the gyro output. The means for generating the output depends on whether the optical instrument is a fiber optic gyro or a ring laser gyro.

Ring Laser Gyros

In a ring laser gyro (RLG), the closed wave-path is implemented using reflecting mirrors (typically 3 or 4) that reflect monochromatic light around a closed optical cavity path [1], [2]. The concept is depicted in Fig. 1.

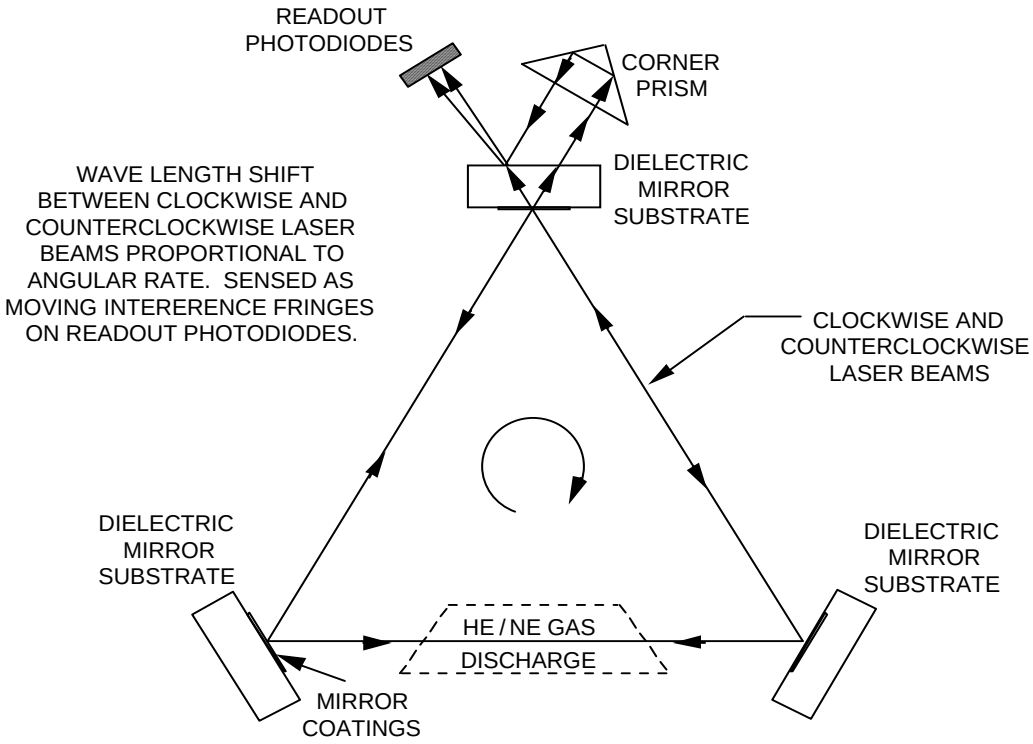

Fig. 1 - Ring Laser Gyro Operating Elements

The monochromatic light in the Fig. 1 light beams is generated by the lasing action of a helium-neon gas laser resident within the closed gyro cavity. As the beams complete each closed circuit between the reflecting mirrors, they collide with the helium-neon lasing plasma, generating new photons in phase and at the same wavelength as the returning photons. The added photons replace those lost during the closed-circuit, creating two oppositely directed never-ending re-circulating beam that begin at gyro turn-on. Consequently, as time increases, the effective beam path length (the total closed-distance traveled by the leading wave since creation at turn-on) becomes progressively longer, and a phase comparison between the oppositely directed beams

thereby represents the total angular rotation (integrated angular rate) experienced since turn-on. Suitable optics built into the RLG combine the counter-rotating beams onto a photo-detector to generate a signal representing the sine of the integrated input angular rate. Each photo-diode output wave thereby signifies rotation through a known angular rotation increment, the basic form of the RLG output.

Fiber Optic Gyros

In a fiber optic gyro (FOG), the closed wave-path is implemented using optical fiber of total length *L* wrapped in several concentric coils, with optical splicing technology used to close, enter, and leave the fiber coil [2]. The concept is depicted in Fig. 2.

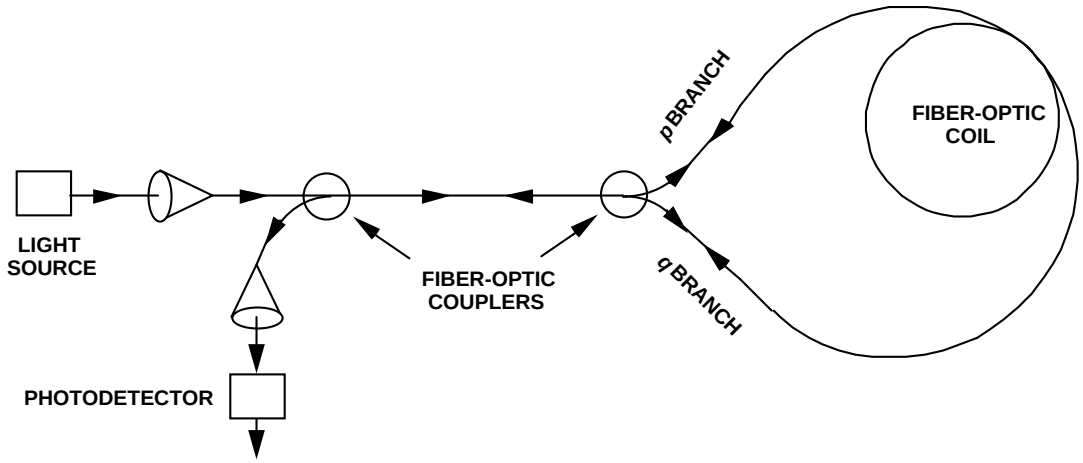

Fig. 2 - Fiber Optic Gyro (FOG) Concept

Monochromatic light within the FOG is generated external to the coil by a super-luminescent diode, and gated through fiber splices into the coil where it splits into the oppositely directed beams (the *p* and *q* branches). When the beams complete the closed-circuit around the coil at *T*, they are gated out of the coil through fiber splices and combined on a photo-detector to measure the angular rotation rate as represented by the sine of the resulting phase difference between the beams. In common practice, the Fig. 2 configuration is augmented by feedback implemented using electro-optic crystals inserted in the fiber circular beam path that change the index of refraction of light passing through [2]. By regulating the refraction indices with electronic feedback commands, the FOG can be operated near pickoff null, thereby eliminating pickoff scale factor errors. Angular rates are then generated from the feedback control loops. Ref. [2] describes the closed-loop FOG concept in detail.

MECHANICAL GYROS

Mechanical gyros implement Newton's basic law of dynamic motion: An applied force to a mass will accelerate the mass in proportion to the force. Original angular rotation sensors were based on the dynamic properties of mechanical gyroscopic instruments, a spinning mass

generating reaction torque to applied inertial rotation. The term "gyro" (for "gyroscope") was used to describe these instruments, a term that has continued to describe forth-coming angular rate sensors based on non-gyroscopic principles. A class of newer technology mechanical angular rate sensors use MEMS (Micro-machined Electro-Mechanical Systems) technology to measure mass reaction forces from vibrating masses generated within a single electronic semi-conductor micro-chip. Each of these mechanical gyro types is described next, showing how they both are based on the same fundamental Eq. (1) kinematic Coriolis principle for sensing angular rotation relative to non-rotating inertial space.

MEMS Type Mechanical Gyros

For a common class of MEMS mechanical gyros, rotating coordinates are affixed to the gyro, $d\underline{\psi}$ in (1) represents a differential angular rotation $d\underline{\theta}$ of the gyro relative to non-rotating inertial space (and the angular increment being sensed); $\underline{\xi}$ in (1) represents a distance vector from linearly vibrating mass q to linearly vibrating mass p within the gyro, both micro-machined into the MEMS silicon substrate, and $d\underline{\xi}$, $d\underline{\Xi}$ represent differential changes in $\underline{\xi}$ that would be measured in non-rotating space ($d\underline{\xi}$) and in the rotating gyro ($d\underline{\Xi}$) during the $d\underline{\psi}$ rotation. Angular rotation produces Coriolis acceleration changes within $d\underline{\xi}$, $d\underline{\Xi}$, which, through Newton's law of dynamic motion, generate reaction forces measured by p and q acceleration sensors (accelerometers) micro-machined into the vibrating masses. Subtracting the p, q accelerometer outputs eliminates their response to linear acceleration, providing an isolated angular rotation induced measurement for output. The associated analytics follows.

Based on the previous discussion, the analytical equivalent of (1) for a MEMS gyro is given by

$$d\underline{x}_{p/q} = d\underline{\chi}_{p/q} + d\underline{\theta} \times \underline{x}_{p/q} \tag{13}$$

where $d\underline{\theta}$ is the differential angular rotation of the gyro relative to non-rotating inertial space (and the angular increment being sensed), $\underline{x}_{p/q}$ is distance vector from point q to point p in the MEMS substrate, each undergoing MEMS generated linear oscillatory motion, $d\underline{x}_{p/q}$ is the vibration induced change in $\underline{x}_{q/a}$ in non-rotating coordinates during the $d\underline{\theta}$ rotation, and $d\underline{\chi}_{p/q}$ is the equivalent of $d\underline{x}_{p/q}$ that would be measured in rotating gyro coordinates during the $d\underline{\theta}$ rotation. For more specificity in the following development, (13) is rewritten as in (A-9):

$$d\underline{x}^I_{p/q} = C^I_B\left(d\underline{\chi}^B_{p/q} + d\underline{\theta}^B_{IB} \times \underline{x}^B_{p/q}\right) \tag{14}$$

where the superscript denotes the projection of the associated vector on "inertial" (I) non-rotating coordinates or "body" (B) rotating coordinates, $d\underline{\theta}^B_{IB}$ is the small angular rotation of the B frame relative to the non-rotating I frame (IB subscript) as projected on B frame axes (superscript), and

C_B^I is the direction cosine matrix that transforms vectors from the *B* frame to the *I* frame. Dividing (14) by the small time interval *dt* for the $d\underline{\theta}_{IB}^B$ rotation finds

$$\frac{d\underline{x}_{p/q}^I}{dt} = C_B^I \left(\frac{d\underline{\chi}_{p/q}^B}{dt} + \frac{d\underline{\theta}_{IB}^B}{dt} \times \underline{x}_{p/q}^B \right) \tag{15}$$

or equivalently,

$$\frac{d\underline{x}_{p/q}^I}{dt} = C_B^I \left(\underline{V}_{p/q}^B + \underline{\omega}_{IB}^B \times \underline{x}_{p/q}^B \right) \tag{16}$$

where $\underline{V}_{p/q}^B$ is the linear velocity of points *p* relative to point *q* in rotating *B* frame coordinates, and $\underline{\omega}_{IB}^B$ is the angular velocity of the *B* frame relative to the non-rotating *I* frame.

Taking the time derivative of (16) using the previous $\underline{V}_{p/q}^B$ definition obtains

$$\frac{d^2\underline{x}_{p/q}^I}{(dt)^2} = \frac{dC_B^I}{dt} \left(\underline{V}_{p/q}^B + \underline{\omega}_{IB}^B \times \underline{x}_{p/q}^B \right) + C_B^I \left(\frac{d\underline{V}_{p/q}^B}{dt} + \frac{d\underline{\omega}_{IB}^B}{dt} \times \underline{x}_{p/q}^B + \underline{\omega}_{IB}^B \times \underline{V}_{p/q}^B \right) \tag{17}$$

From [4, Eq. (3.3.2-6)], $\frac{dC_B^I}{dt} = C_B^I \left(\underline{\omega}_{IB}^B \times \right)$, for which (17) becomes

$$\frac{d^2\underline{x}_{p/q}^I}{(dt)^2} = C_B^I \left[\underline{\omega}_{IB}^B \times \left(\underline{\omega}_{IB}^B \times \underline{x}_{p/q}^B \right) + \frac{d\underline{\omega}_{IB}^B}{dt} \times \underline{x}_{p/q}^B + 2\,\underline{\omega}_{IB}^B \times \underline{V}_{p/q}^B + \frac{d\underline{V}_{p/q}^B}{dt} \right] \tag{18}$$

Ref. [5, Eqs. (15) - (16)] shows that

$$\frac{d^2\underline{x}_{p/q}^I}{(dt)^2} = \underline{a}_{SF\,p}^I - \underline{a}_{SF\,q}^I + \underline{g}_p^I - \underline{g}_q^I \tag{19}$$

where $\underline{a}_{SF\,p}^I$, $\underline{a}_{SF\,q}^I$ are the non-gravitational specific force accelerations at points *p* and *q* (i.e., the accelerations that would be measured by *p* and *q* located accelerometers), and $\underline{g}_p^I$, $\underline{g}_q^I$ are the gravitational accelerations at these points. Accelerometers implement Newton's first and second laws of motion: 1) Every action is accompanied by an equal and opposite reaction, and 2) Applied

force to a mass generates a mass acceleration proportional to the mass. For masses fixed to points p and q, the reaction to the p, q motion on the p, q masses are forces proportional to the masses. Accelerometers measure the generated p, q forces, hence, measure $\underline{a}^I_{SF\,p}$, $\underline{a}^I_{SF\,q}$ in (19).

Substituting (19) in (18) while assuming that points p and q are sufficiently close that $\underline{g}^I_q \approx \underline{g}^I_p$ yields

$$\underline{a}^I_{SF\,p} - \underline{a}^I_{SF\,q} = C^I_B\left[\underline{\omega}^B_{IB}\times\left(\underline{\omega}^B_{IB}\times\underline{x}^B_{p/q}\right) + \frac{d\,\underline{\omega}^B_{IB}}{dt}\times\underline{x}^B_{p/q} + 2\,\underline{\omega}^B_{IB}\times\underline{V}^B_{p/q} + \frac{d\underline{V}^B_{p/q}}{dt}\right] \quad (20)$$

Lastly, multiplying (20) by the C^I_B inverse obtains

$$\underline{a}^B_{SF\,p} - \underline{a}^B_{SF\,q} = \underline{\omega}^B_{IB}\times\left(\underline{\omega}^B_{IB}\times\underline{x}^B_{p/q}\right) + \frac{d\,\underline{\omega}^B_{IB}}{dt}\times\underline{x}^B_{p/q} + 2\,\underline{\omega}^B_{IB}\times\underline{V}^B_{p/q} + \frac{d\underline{V}^B_{p/q}}{dt} \quad (21)$$

Since all vectors in (21) are in B frame coordinates, a simplified form of (9) is

$$\underline{a}_{SF\,p} - \underline{a}_{SF\,q} = \underline{\omega}\times\left(\underline{\omega}\times\underline{x}_{p/q}\right) + \frac{d\,\underline{\omega}}{dt}\times\underline{x}_{p/q} + 2\,\underline{\omega}\times\underline{V}_{p/q} + \frac{d\underline{V}_{p/q}}{dt} \quad (22)$$

in which all vectors are evaluated in a coordinate frame that rotates with the body and $\underline{\omega}$ is the body angular rate relative to non-rotating inertial space.

Eq. (22) represents a general form applicable to MEMS gyros having points p and q separated by distance vector $\underline{x}_{p/q}$, each driven into linear oscillation at $\underline{V}_{p/q}$ relative velocity (p relative to q), $\underline{a}_{SF\,p}$ and $\underline{a}_{SF\,q}$ are specific forces at points p and q measured by MEMS accelerometers at these locations, and $\underline{\omega}$ is the inertial angular rate to be measured. The MEMS p, q accelerometers are configured to have parallel input axes perpendicular to $\underline{x}_{p/q}$.

For a typical MEMS gyro configuration, points p and q (and their associated accelerometers) are driven in opposite directions into linear oscillation along the $\underline{x}_{p/q}$ line, a line that is fixed within the rotating gyro. We then define a set of mutually orthogonal unit vectors as

$$\begin{aligned} &\underline{u}_{p/q} \equiv \text{ Parallel to } \underline{x}_{p/q}, \text{ i.e., } \underline{x}_{p/q} = x_{p/q}\,\underline{u}_{p/q} \quad \therefore \underline{V}_{p/q} = V_{p/q}\,\underline{u}_{p/q} \\ &\underline{u}_{aInpt} \equiv \text{ Accelerometers Input Axis} \quad \underline{u}_{\omega Inpt} \equiv \underline{u}_{p/q}\times\underline{u}_{aInpt} = \text{Gyro Input Axis} \end{aligned} \quad (23)$$

where $\underline{u}_{p/q}$ is fixed within the rotating gyro in the direction of $\underline{x}_{p/q}$, $x_{p/q}$ is the magnitude of $\underline{x}_{p/q}$, $\underline{V}_{p/q}$ is parallel to $\underline{x}_{p/q}$, $V_{p/q}$ is the signed magnitude of $V_{p/q}$, and $\underline{u}_{\omega Inpt}$ is the gyro input axis. With these definitions we now take the dot product of (22) with $\underline{u}_{aInpt}$ to obtain

$$\begin{aligned}
\underline{u}_{aInpt}\cdot\left(\underline{a}_{SF\,p}-\underline{a}_{SF\,q}\right) &= \underline{u}_{aInpt}\cdot\left[\underline{\omega}\times\left(\underline{\omega}\times\underline{x}_{p/q}\right)\right]+\underline{u}_{aInpt}\cdot\left(\frac{d\underline{\omega}}{dt}\times\underline{x}_{p/q}\right)\\
&\quad +2\,\underline{u}_{aInpt}\cdot\left(\underline{\omega}\times\underline{V}_{p/q}\right)+\underline{u}_{aInpt}\cdot\frac{d\underline{V}_{p/q}}{dt}\\
&= x_{p/q}\,\underline{u}_{aInpt}\cdot\left[\underline{\omega}\left(\underline{\omega}\cdot\underline{u}_{p/q}\right)-\underline{u}_{p/q}\,\omega^2\right]+x_{p/q}\left(\underline{u}_{p/q}\times\underline{u}_{aInpt}\right)\cdot\frac{d\underline{\omega}}{dt} \qquad (24)\\
&\quad +2\,V_{p/q}\left(\underline{u}_{p/q}\times\underline{u}_{aInpt}\right)\cdot\underline{\omega}+\underline{u}_{aInpt}\cdot\underline{u}_{p/q}\frac{dV_{p/q}}{dt}\\
&= x_{p/q}\left[\left(\underline{u}_{aInpt}\cdot\underline{\omega}\right)\left(\underline{u}_{p/q}\cdot\underline{\omega}\right)+\underline{u}_{\omega Inpt}\cdot\frac{d\underline{\omega}}{dt}\right]+2\,V_{p/q}\,\underline{u}_{\omega Inpt}\cdot\underline{\omega}
\end{aligned}$$

where ω is the magnitude of $\underline{\omega}$. If the MEMS generated signed $V_{p/q}$ velocity is a sine function of time, the $x_{p/q}$ value in (24) will be a small cosine oscillation (i.e., in quadrature with $V_{p/q}$) plus a constant. For $\underline{u}_{aInpt}\cdot\left(\underline{a}_{SF\,p}-\underline{a}_{SF\,q}\right)$ sampled with a phase sensitive demodulator synchronized with $V_{p/q}$, the $\left[\left(\underline{u}_{aInpt}\cdot\underline{\omega}\right)\left(\underline{u}_{p/q}\cdot\underline{\omega}\right)+\underline{u}_{\omega Inpt}\cdot\frac{d\underline{\omega}}{dt}\right]$ coefficient in (24) will be eliminated and the demodulated output will be

$$\left[\underline{u}_{aInpt}\cdot\left(\underline{a}_{SF\,p}-\underline{a}_{SF\,q}\right)\right]_{demod}=2\left|V_{p/q}\right|\underline{u}_{\omega Inpt}\cdot\underline{\omega} \qquad (25)$$

where $\left|V_{p/q}\right|$ is the unsigned magnitude of $\underline{V}_{p/q}$. The resulting MEMS gyro output will then be

$$\underline{u}_{\omega Inpt}\cdot\underline{\omega}=\left[\underline{u}_{aInpt}\cdot\left(\underline{a}_{SF\,p}-\underline{a}_{SF\,q}\right)\right]_{demod}/\left(2\left|V_{p/q}\right|\right) \qquad (26)$$

Fig. 3 depicts a MEMS gyro designed at the Charles Stark Draper Laboratory to implement (26). A version of the unit is in production at Honeywell Minneapolis. The Fig. 3 configuration is but one of several silicon MEMS devices developed for angular rate sensing. The same fundamental principal of operation for each is represented by (21): Angular rate is sensed through kinematic generated Coriolis acceleration producing a reaction force on driven vibrating mass. The configurations differ in their physical structure and mechanism for creating the vibration and for sensing the Coriolis reaction force.

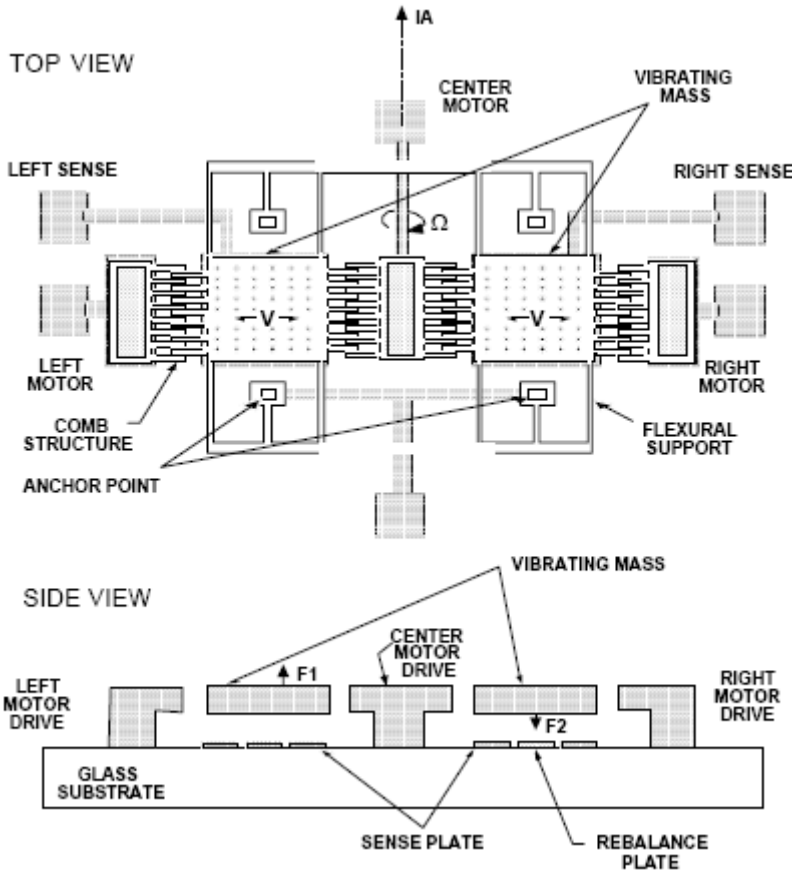

Fig. 3 – Representative MEMS Gyro Configuration

The Fig. 3 MEMS gyro configuration consists of a silicon structure mounted to a glass substrate with deposited metallization for sensor interfacing. The silicon structure is micro-machined to contain two masses suspended by a sequence of beams anchored to the substrate in an arrangement characterized as a double ended tuning fork. By applying oscillatory voltages to the outer motor drives, the two masses are electro-statically forced through a comb structure into lateral in-plane velocity oscillations V. The comb structure provides added surface area to magnify the electrostatic driving force.

Each motor drive control loop is a self-drive oscillator using proof mass position feedback to sustain constant proof mass motion amplitude. The linear proof mass motion creates oscillating in-plane linear momentum that rotates under applied input axis angular rate Ω. Rotation of the oscillating linear momentum vectors generates oscillating reaction forces (F_1 and F_2) through the Coriolis effect (i.e., rotating a linear momentum vector requires applied force perpendicular to the momentum and rotation rate vectors). The oscillating Coriolis reaction forces are equal but opposite for each mass (because the linear momentum of each is opposite the other) which produces out of plane differential oscillations of the masses with amplitude directly proportional to applied angular rate and inversely proportional to the silicon suspension stiffness.

The out-of-plane oscillation is measured by capacitor plate pickoffs under each of the two masses, generating an oscillatory electrical signal proportional to applied angular rate. The

oscillatory angular rate signal is then demodulated for output using a reference voltage generated in the motor drive control loop. For improved accuracy, electrostatic oscillatory closed-loop control can be employed to maintain the masses at null, thereby reducing the effect of pickoff scale factor and silicon structure stiffness uncertainty as error sources. The closed-loop control voltage amplitude would then be used as the measured angular rate signal.

Momentum Wheel Type Mechanical Gyros

A classical momentum wheel gyro consists of a spinning rotor "wheel" contained within a closed housing [1]. The housing is mounted within the gyro case using a suspension mechanism that allows only known torques (differential equal magnitude forces operating at opposite ends of a lever arm) to be applied to the housing, perpendicular to axes for which case angular rate is to be measured. The governing equation for the gyro is (1) for which $d\underline{\psi}$ represents an infinitesimally small angular change in the housing angular orientation relative to non-rotating inertial space, $\underline{\xi}$ represents the angular momentum of the housing including that of the enclosed spinning rotor, $d\underline{\xi}$ represents, the change in angular momentum components during the $d\underline{\psi}$ rotation that would be measured in non-rotating inertial space, and $d\underline{\Xi}$ represents the change in angular momentum components during the $d\underline{\psi}$ rotation that would be measured in a coordinate frame rotating with the rotor housing. For more specificity, the momentum wheel gyro equivalent to (1) can be rewritten as in (A-9) of Appendix A:

$$d\underline{h}^I_{hsng+rtr/a} = C^I_B\left(d\underline{H}^B_{hsng+rtr/a} + d\underline{\theta}^B_{IB}\times\underline{H}^B_{hsng+rtr/a}\right) \qquad (27)$$

where the superscripts represent the coordinate frame in which the vector components are being measured, *I* for the inertially non-rotating frame, *B* for the frame that rotates with the gyro rotor housing, the *IB* subscript denotes rotation of the *B* frame relative to the *I* frame, C^I_B is the direction cosine matrix that transforms vector projections from the *B* frame to the *I* frame, and subscript $hsng + rtr / a$ denotes the angular momentum of the gyro rotor housing (including the rotor) around its center of mass point *a*. Dividing (27) by the time interval *dt* for the $d\underline{\theta}^B_{IB}$ rotation obtains the differential equation

$$\frac{d\underline{h}^I_{hsng+rtr/a}}{dt} = C^I_B\left(\frac{d\underline{H}^B_{hsng+rtr/a}}{dt} + \underline{\omega}^B_{IB}\times\underline{H}^B_{hsng+rtr/a}\right) \qquad (28)$$

where $\underline{\omega}^B_{IB}$ is the angular rate of the rotor housing relative to non-rotating inertial space, i.e., $\underline{\omega}^B_{IB} \equiv d\underline{\theta}^B_{IB}/dt$.

Eq. (B-10) in Appendix B shows that $\frac{d\underline{h}^I_{hsng+rtr/a}}{dt}$ in (28) equals the composite of *k* external torques $\underline{T}^I_k$ applied to the rotor housing:

$$\frac{d\,\underline{h}^I_{hsng+rtr}}{dt} = \sum_k \underline{T}^I_k \tag{29}$$

Appendix B, Eq. (B-2) shows that the rotor housing plus rotor angular momentum around its center of mass (point *a*) is defined in *I* frame coordinates as

$$\underline{h}^I_{hsng+rtr/a} = \int_i \left(\underline{r}^I_{i/a} \times \frac{d\,\underline{r}^I_{i/a}}{dt} \right) \rho_i \, dv \tag{30}$$

where $\underline{r}^I_{i/a}$ is the distance from the housing+rotor center of mass point *a* to point *i* in the housing+rotor, ρ_i is the mass density at point *i*, and *dv* is a differential volume at point *i*. The angular momentum vector in *B* frame coordinates $\underline{H}^B_{hsng+rtr/a}$ equals $\underline{h}^I_{hsng+rtr/a}$ in (30) transformed to the *B* frame:

$$\begin{aligned} \underline{H}^B_{hsng+rtr/a} &= C^B_I \, \underline{h}^I_{hsng+rtr/a} = C^B_I \int_i \left(\underline{r}^I_{i/a} \times \frac{d\,\underline{r}^I_{i/a}}{dt} \right) \rho_i \, dv \\ &= \int_i \left[C^B_I \, \underline{r}^I_{i/a} \, C^I_B \, C^B_I \left(\frac{d\,\underline{r}^I_{i/a}}{dt} \right) \right] \rho_i \, dv = \int_i \left[\left(\underline{r}^B_{i/a} \times \right) C^B_I \left(\frac{d\,\underline{r}^I_{i/a}}{dt} \right) \right] \rho_i \, dv \end{aligned} \tag{31}$$

Ref. [4, Eq. (3.4-6)] transformed to the *B* frame finds for the $C^B_I \left(\frac{d\,\underline{r}^I_{i/a}}{dt} \right)$ term in (31):

$$C^B_I \left(\frac{d\,\underline{r}^I_{i/a}}{dt} \right) = \frac{d\,\underline{r}^B_{i/a}}{dt} + \underline{\omega}^B_{IB} \times \underline{r}^B_{i/a} \tag{32}$$

Substituting (32) in (31) obtains

$$\begin{aligned} \underline{H}^B_{hsng+rtr/a} &= \int_i \left[\left(\underline{r}^B_{i/a} \times \right) \left(\frac{d\,\underline{r}^B_{i/a}}{dt} + \underline{\omega}^B_{IB} \times \underline{r}^B_{i/a} \right) \right] \rho_i \, dv \\ &= \int_i \left[\left(\underline{r}^B_{i/a} \times \right) \underline{\omega}^B_{IB} \times \underline{r}^B_{i/a} \right] \rho_i \, dv + \int_i \left[\left(\underline{r}^B_{i/a} \times \right) \frac{d\,\underline{r}^B_{i/a}}{dt} \right] \rho_i \, dv \\ &= -\left\{ \int_i \left[\left(\underline{r}^B_{i/a} \times \right) \left(\underline{r}^B_{i/a} \times \right) \right] \rho_i \, dv \right\} \underline{\omega}^B_{IB} + \int_i \left[\left(\underline{r}^B_{i/a} \times \right) \frac{d\,\underline{r}^B_{i/a}}{dt} \right] \rho_i \, dv \end{aligned} \tag{33}$$

For the *i* points located in the rigid housing (i.e., not in the rotor), $\underline{r}^B_{i/a}$ is constant, hence, the second integral in (33) for these points is zero. For the remaining *i* points (i.e., those in the rotor), identify them as *j* points so that (33) becomes

$$\underline{H}^B_{hsng+rtr/a} = -\left\{\int_i \left[\left(\underline{r}^B_{i/a}\times\right)\left(\underline{r}^B_{i/a}\times\right)\right]\rho_i\, dv\right\}\underline{\omega}^B_{IB} + \int_j \left[\left(\underline{r}^B_{j/a}\times\right)\frac{d\,\underline{r}^B_{j/a}}{dt}\right]\rho_j\, dv \qquad (34)$$

Define

$$\underline{r}^B_{j/a} = \underline{r}^B_{b/a} + \underline{r}^B_{j/b} \qquad (35)$$

where $\underline{r}^B_{b/a}$ is the distance vector from point *a* (the housing+rotor center of mass) to the rotor center of mass at point *b*, and $\underline{r}^B_{j/b}$ is the distance vector from point *b* to point *j* in the rotor. For a symmetrical rotor, the rotor center of mass location *b* will be fixed in the housing. Then $\underline{r}^B_{b/a}$ will be constant so that the integrand in the second (34) integral becomes

$$\left(\underline{r}^B_{j/a}\times\right)\frac{d\,\underline{r}^B_{j/a}}{dt} = \left[\left(\underline{r}^B_{b/a} + \underline{r}^B_{j/b}\right)\times\right]\frac{d\,\underline{r}^B_{j/b}}{dt} = \underline{r}^B_{b/a}\times\frac{d\,\underline{r}^B_{j/b}}{dt} + \underline{r}^B_{j/b}\times\frac{d\,\underline{r}^B_{j/b}}{dt} \qquad (36)$$

Now identify another coordinate frame *R* that rotates with the spinning rotor. Recognizing that $\underline{r}^R_{j/b}$ is constant in the *R* frame, the general Coriolis relationship [4, Eq. (3.4-6)] shows that

$$\frac{d\,\underline{r}^B_{j/b}}{dt} = C^B_R\frac{d\,\underline{r}^R_{j/b}}{dt} + \underline{\omega}^B_{BR}\times\underline{r}^B_{j/b} = \underline{\omega}^B_{BR}\times\underline{r}^B_{j/b} \qquad (37)$$

where $\underline{\omega}^B_{BR}$ is the angular rate of the rotor fixed *R* frame relative to the rotating *B* frame. Substituting (37) in (36) obtains

$$\begin{aligned}\left(\underline{r}^B_{j/a}\times\right)\frac{d\,\underline{r}^B_{j/a}}{dt} &= \underline{r}^B_{b/a}\times\left(\underline{\omega}^B_{BR}\times\underline{r}^B_{j/b}\right) + \underline{r}^B_{j/b}\times\left(\underline{\omega}^B_{BR}\times\underline{r}^B_{j/b}\right)\\ &= \left(\underline{r}^B_{b/a}\times\right)\left(\underline{\omega}^B_{BR}\times\right)\underline{r}^B_{j/b} - \left(\underline{r}^B_{j/b}\times\right)\left(\underline{r}^B_{j/b}\times\right)\underline{\omega}^B_{BR}\end{aligned} \qquad (38)$$

With (38), the second integral term in (34) becomes

$$\int_j \left[\left(\underline{r}^B_{j/a} \times \right) \frac{d\underline{r}^B_{j/a}}{dt} \right] \rho_j \, dv$$

$$= \int_j \left(\underline{r}^B_{b/a} \times \right) \left(\underline{\omega}^B_{BR} \times \right) \underline{r}^B_{j/b} \, \rho_j \, dv - \int_j \left(\underline{r}^B_{j/b} \times \right) \left(\underline{r}^B_{j/b} \times \right) \underline{\omega}^B_{BR} \, \rho_j \, dv \qquad (39)$$

$$= \left(\underline{r}^B_{b/a} \times \right) \left(\underline{\omega}^B_{BR} \times \right) \int_j \underline{r}^B_{j/b} \, \rho_j \, dv - \left[\int_j \left(\underline{r}^B_{j/b} \times \right) \left(\underline{r}^B_{j/b} \times \right) \rho_j \, dv \right] \underline{\omega}^B_{BR}$$

Since point *b* was defined as the rotor center of mass, $\int_j \underline{r}^B_{j/b} \, \rho_j \, dv = 0$, and (39) simplifies to

$$\int_j \left[\left(\underline{r}^B_{j/a} \times \right) \frac{d\underline{r}^B_{j/a}}{dt} \right] \rho_j \, dv = -\left[\int_j \left(\underline{r}^B_{j/b} \times \right) \left(\underline{r}^B_{j/b} \times \right) \rho_j \, dv \right] \underline{\omega}^B_{BR} \qquad (40)$$

Then with (40), (34) becomes

$$\underline{H}^B_{hsng+rtr/a} = -\left[\int_i \left(\underline{r}^B_{i/a} \times \right) \left(\underline{r}^B_{i/a} \times \right) \rho_i \, dv \right] \underline{\omega}^B_{IB} - \left[\int_j \left(\underline{r}^B_{j/b} \times \right) \left(\underline{r}^B_{j/b} \times \right) \rho_j \, dv \right] \underline{\omega}^B_{BR} \qquad (41)$$

Define

$$J^B_{hsng+rtr/a} \equiv -\int_i \left(\underline{r}^B_{i/a} \times \right) \left(\underline{r}^B_{i/a} \times \right) \rho_i \, dv \qquad J^B_{rtr/b} \equiv -\int_j \left(\underline{r}^B_{j/b} \times \right) \left(\underline{r}^B_{j/b} \times \right) \rho_j \, dv \qquad (42)$$

where $J^B_{hsng+rtr/a}$ is the moment of inertia tensor of the housing+rotor assembly about its center-of-mass point *a* as measured in *B* frame coordinates, and $J^B_{rtr/b}$ is the *B* frame measured moment of inertia tensor of the rotor about its center-of-mass point *b*. With the (42) definitions, (41) assumes the simpler form

$$\underline{H}^B_{hsng+rtr/a} = J^B_{hsng+rtr/a} \, \underline{\omega}^B_{IB} + J^B_{rtr/b} \, \underline{\omega}^B_{BR} \qquad (43)$$

For the derivative of (43) in (28), assume that the rotor speed $\underline{\omega}^B_{BR}$ is maintained constant by the synchronous hysteresis spin-motor drive so that $\frac{d\underline{\omega}^B_{BR}}{dt} = 0$. Additionally, assuming a symmetrical rotor, $J^B_{hsng+rtr/a}$ and $J^B_{rtr/b}$ will be constant, hence

$$\frac{d\underline{H}^B_{hsng+rtr/a}}{dt} = J^B_{hsng+rtr/a} \frac{d\underline{\omega}^B_{IB}}{dt} \qquad (44)$$

Lastly, substitute (43), (44), and (29) in (28), and transform to the *B* frame for the final result:

$$\sum_k \underline{T}_k^B = \underline{\omega}_{IB}^B \times \left(J_{rtr/b}^B \, \underline{\omega}_{BR}^B \right) + J_{hsng+rtr/a}^B \frac{d\,\underline{\omega}_{IB}^B}{dt} + \underline{\omega}_{IB}^B \times \left(J_{hsng+rtr/a}^B \, \underline{\omega}_{IB}^B \right) \qquad (45)$$

Eq. (45) is a general result applicable to several momentum wheel gyro configurations. As a particular example of (45), the remainder of this section will describe the single-degree-of-freedom (SDOF) floated rate-integrating gyro as described pictorially in Fig. 4.

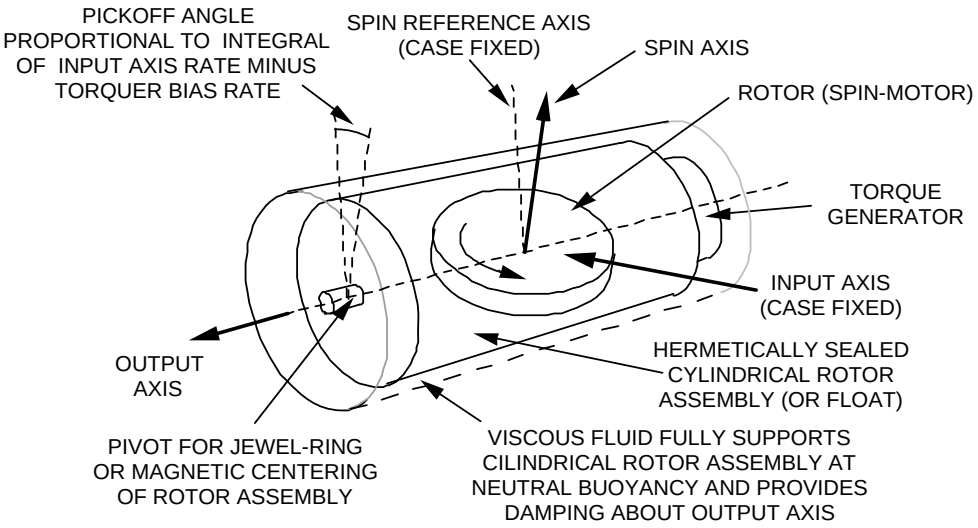

Fig. 4 – Single Degree of Freedom Inertial Rate Integrating Gyro

The SDOF gyro configuration depicted in Fig. 4 consists of a cylindrical hermetically sealed momentum-wheel/spin-motor assembly (float) contained in a cylindrical hermetically sealed case. The float is interfaced to the case by a precision suspension assembly that is laterally rigid (normal to the cylinder case) but allows "frictionless" angular movement of the float relative to the case about the cylinder axis. The cavity between the case and float is filled with a fluid that serves the dual purpose of suspending the float at neutral buoyancy, and providing viscous damping to resist relative float-case angular motion about the suspension axis (output axis).

A ball-bearing or gas-bearing synchronous-hysteresis spin-motor is utilized in the float to maintain constant rotor spin-speed, hence constant float angular momentum. An electrical pickoff assembly provides an electrical output signal from the gyro proportional to the angular displacement of the float relative to the case. An electrical torque generator (typically a torquer coil on the float and a permanent magnet on the case) provides the capability for applying known torques to the float about the suspension axis proportional to an applied electrical input current. Delicate flex leads are used to transmit electrical signals and power between the case and float.

Under applied angular rates about the input axis, the gyro float develops a precessional rate about the output axis (rotation rate of the angle sensed by the pick-off). The pick-off angle rate generates viscous torque on the float about the output axis (due to the damping fluid) which sums with the electrically applied torque-generator torque to precess the float about the input axis at the gyro input rate. The pick-off angle rate thereby becomes proportional to the difference between the input rate and the torque generator precessional rate; hence, the pickoff angle

becomes proportional to the integral of the difference between the input and torque-generator rates (thus, the name rate-integrating gyro).

To operate the gyro in a gimbaled application, three gyros are mounted (with input axes orthogonal to one-another) on a "platform" that is physically supported by gimbals which are electro-mechanically controlled by "gimbal torque motors" positioned around the gimbal axes. The drive signals to the gimbal torquers are designed to maintain the gyro pickoff angles at null. Desired rotation rates of the platform (as specified by the inertial system computer) are used as "gyro torque generator" inputs. By maintaining the gyro outputs at null (i.e., the integrated difference between the computer command rates and actual platform rotation rates), the platform rate is forced to balance the computer command rate (in the integral sense).

To operate the gyro in a strapdown mode, the pickoff angle is electrically servoed to null by the gyro torque generator which is driven by the pickoff output signal. The time integral of the difference between the input inertial angular rate and torque-generator rate is thereby maintained at zero, and the integral of the torque-generator electrical current measures the integral of the gyro input rate for the strapdown inertial system computer.

To analytically describe the SDOF floated rate integrating gyro, we apply (45) to Fig. 4, identifying x as the "Input Axis", y as the "Output Axis", and z as the "Spin Reference Axis". Assuming no cross-products of inertia for the float assembly and rotor, these definitions find

$$J^B_{hsng+rtr/a} \equiv \begin{bmatrix} J_{x\,Float} & 0 & 0 \\ 0 & J_{y\,Float} & 0 \\ 0 & 0 & J_{z\,Float} \end{bmatrix} \quad J^B_{rtr/b} \equiv \begin{bmatrix} J_{Crs\,Rtr} & 0 & 0 \\ 0 & J_{Crs\,Rtr} & 0 \\ 0 & 0 & J_{Spn\,Rtr} \end{bmatrix}$$
$$\underline{\omega}^B_{IB} \equiv \begin{bmatrix} \omega_{IB\,Input} \\ \omega_{IB\,Output} \\ \omega_{IB\,Spn} \end{bmatrix} \quad \underline{\omega}^B_{BR} \equiv \begin{bmatrix} 0 \\ 0 \\ \omega_{BR\,Spn} \end{bmatrix} \tag{46}$$

where $J_{Crs\,Rtr}$ is the rotor moment of inertia around any axis perpendicular to the spin axis, $J_{Spn\,Rtr}$ is the rotor moment of inertia around the spin axis, and $\omega_{BR\,Spn}$ is the rotor spin rate relative to the float assembly. Substituting (46) into (45) obtains for the components along the output (y) axis:

$$\begin{aligned} T_{Net} &= -J_{Spin\,Rtr}\,\omega_{BR\,Spn}\,\omega_{IB\,Input} \\ &+ J_{y\,Float}\frac{d\,\omega_{IB\,Output}}{dt} + \left(J_{x\,Float} - J_{z\,Float}\right)\omega_{IB\,Input}\,\omega_{IB\,Spn} \end{aligned} \tag{47}$$

where T_{Net} is the net torque $\sum_k \underline{T}_k^B$ component in (45) around the Fig. 4 gyro output axis. The net torque is composed of three terms, viscous floatation fluid torque proportional to the rate of change of the angle ϕ between the float and case, specified command torque T_{Cmd} electrically input through the gyro torque generator, and extraneous error torques T_{Err}:

$$T_{Net} = -c\frac{d\phi}{dt} - T_{Cmd} - T_{Err} \tag{48}$$

Substituting (48) in (47) yields after rearrangement

$$\begin{aligned} c\frac{d\phi}{dt} &= J_{Spin_{Rtr}}\,\omega_{BR_{Spn}}\,\omega_{IB_{Input}} - T_{Cmd} - T_{Err} \\ -J_{y_{Float}}\frac{d\omega_{IB_{Output}}}{dt} &- \left(J_{x_{Float}} - J_{z_{Float}}\right)\omega_{IB_{Input}}\,\omega_{IB_{Spn}} \end{aligned} \tag{49}$$

Further clarifying, define

$$J_{Spn_{Rtr}}\,\omega_{BR_{Spn}} = H_{BR_{Rtr}} \qquad T_{Cmd} = H_{BR_{Rtr}}\,\omega_{Cmd} \qquad T_{Err} = H_{BR_{Rtr}}\,\omega_{Err} \tag{50}$$

with which the integral of (49) becomes for the gyro pickoff angle output:

$$\phi = \int \frac{H_{BR_{Rtr}}}{c}\left[\begin{array}{c} \omega_{IB_{Input}} - \omega_{Cmd} \\ -\omega_{Err} - \dfrac{J_{y_{Float}}}{H_{BR_{Rtr}}}\dfrac{d\omega_{IB_{Output}}}{dt} - \dfrac{\left(J_{x_{Float}} - J_{z_{Float}}\right)}{H_{BR_{Rtr}}}\omega_{IB_{Input}}\,\omega_{IB_{Spn}} \end{array}\right] dt \tag{51}$$

Due to the large value of $H_{BR_{Rtr}}$ (from the high gyro rotor spin rate) and the relative smallness of ω_{Err} (compared with $\omega_{IB_{Input}}$), the $\omega_{IB_{Input}} - \omega_{Cmd}$ term dominates the bracketed terms in (51). Thus, for a gimbaled system, maintaining the gyro readout angle ϕ near zero (by mechanical gimbal torque command feedback), the platform integrated inertial angular rate $\omega_{IB_{Input}}$ will equal the integrated gyro torque generator command rate ω_{Cmd}. For a strapdown system, maintaining the gyro readout angle ϕ near zero (by electrical feedback from the gyro pickoff through the gyro torque generator), the integrated ω_{Cmd} torque generator input will equal the true angular rate input $\omega_{IB_{Input}}$ to the gyro, hence, serve as the gyro output measure of measure inertial angular rate.

CONCLUSIONS

Both optical and mechanical angular rate sensors are based on the same kinematic principle: The components of a vector measured in an inertially non-rotating coordinate frame equal its

component measurements in a rotating frame plus a Coriolis correction proportional to the angular rate relative to non-rotating inertial space. Optical and mechanical gyros are based on different fundamental laws of physics, each law being valid in inertially non-rotating coordinates; optical gyros are based on the Einstein's constant-speed-of-light Relativity principle; mechanical gyros are based on the Newtonian dynamic mass response to applied force principle. Having these fundamental laws valid in non-rotating coordinates provides the means for translating their effect into rotating coordinates through the same common Coriolis kinematic equation. The result is that both optical and mechanical gyros measure the same angular rate relative to inertially non-rotating coordinates.

APPENDIX A

FUNDAMENTAL INERTIAL ANGULAR MEASUREMENT EQUATION

Consider an inertially non-rotating coordinate reference frame I. Further, consider two other inertially non-rotating coordinate frames B_1 and B_2 defined as parallel to the instantaneous orientation of rotating coordinate frame B at successive time instants t_1 and t_2. Because B_1 and B_2 are non-rotating relative to a common non-rotating space, the angular orientation of B_2 relative to B_1, and B_1 relative to I will be constant. Now, define an arbitrary vector $\underline{\xi}$, and $\underline{\xi}_1^I$, $\underline{\xi}_2^I$, $\underline{\xi}_1^{B1}$, $\underline{\xi}_2^{B1}$, $\underline{\xi}_1^{B2}$, $\underline{\xi}_2^{B2}$, the projections of $\underline{\xi}$ on the I, B_1, and B_2 coordinate axes (superscripts) at time instants t_1 and t_2 (subscripts 1 and 2). Considering C_{B2}^{B1} as a direction cosine matrix transforms vectors from frame B_2 to B_1, and C_{B1}^{I} as a direction cosine matrix that transforms vectors from frame B_1 to I, we can write

$$\underline{\xi}_1^I = C_{B1}^I \underline{\xi}_1^{B1} \qquad \underline{\xi}_2^I = C_{B1}^I C_{B2}^{B1} \underline{\xi}_2^{B2} \tag{A-1}$$

Also define the difference between the $\underline{\xi}$ values at t_1 and t_2 as

$$\Delta\underline{\xi}^I \equiv \underline{\xi}_2^I - \underline{\xi}_1^I \qquad \Delta\underline{\Xi}^{B1} \equiv \underline{\xi}_2^{B2} - \underline{\xi}_1^{B1} \tag{A-2}$$

where $\Delta\underline{\xi}^I$ is the change in $\underline{\xi}$ that would be measured in non-rotating frame I and $\Delta\underline{\Xi}^{B1}$ is the change in $\underline{\xi}$ that would be measured in the rotating B frame over time instants t_1 and t_2. Then, based on (A-1) and (A-2):

$$\begin{aligned} \Delta\underline{\xi}^I &= \underline{\xi}_2^I - \underline{\xi}_1^I = C_{B1}^I C_{B2}^{B1} \underline{\xi}_2^{B2} - C_{B1}^I \underline{\xi}_1^{B1} \\ &= \left(C_{B1}^I C_{B2}^{B1} - C_{B1}^I\right)\underline{\xi}_2^{B2} + C_{B1}^I \underline{\xi}_2^{B2} - C_{B1}^I \underline{\xi}_1^{B1} = C_{B1}^I\left[\left(C_{B2}^{B1} - I\right)\underline{\xi}_2^{B2} + \Delta\underline{\Xi}^{B1}\right] \end{aligned} \tag{A-3}$$

For $C_{B_2}^{B_1}$ representing a small angular rotation $\Delta\underline{\psi}_{IB}^{B}$ over time interval t_1 to t_2, [4, Eqs. (3.5.2-10 & (3.5.2-17)] shows that

$$C_{B_2}^{B_1} - I \approx \left(\Delta\underline{\psi}_{IB}^{B}\times\right) \tag{A-4}$$

where the *IB* subscript indicates the angular rotation of frame *B* from its orientation parallel to non-rotating inertial frame B_1 to its orientation parallel to non-rotating inertial frame B_2. Substituting (A-4) in (A-3) obtains

$$\Delta\underline{\xi}^{I} = C_{B_1}^{I}\left[\Delta\underline{\Xi}^{B_1} + \left(\Delta\underline{\psi}_{IB}^{B}\times\right)\underline{\xi}_{2}^{B_2}\right] = C_{B_1}^{I}\left(\Delta\underline{\Xi}^{B_1} + \Delta\underline{\psi}_{IB}^{B}\times\underline{\xi}_{2}^{B_2}\right) \tag{A-5}$$

We then let the Δ changes become very small so that during the t_1 to t_2 time interval, Eq. (A-5) vector projections on the B_1 and B_2 frames can be approximated by their projections on the *B* frame in general, and $\underline{\xi}_{2}^{B_2}$ can be approximated by its value in general: $\underline{\xi}_{2}^{B_2} \to \underline{\xi}^{B}$, $\Delta\underline{\xi}^{B_1} \to \Delta\underline{\xi}^{B}$, $\Delta\underline{\Xi}^{B_1} \to \Delta\underline{\Xi}^{B}$, $C_{B_1}^{I} \to C_{B}^{I}$. Thus, (A-5) becomes

$$\Delta\underline{\xi}^{I} = C_{B}^{I}\left(\Delta\underline{\Xi}^{B} + \Delta\underline{\psi}_{IB}^{B}\times\underline{\xi}^{B}\right) \tag{A-6}$$

Multiplying by C_{I}^{B} (the direction cosine matrix that transforms vectors from the *I* to the *B* frame) transforms (A-6) to the B frame:

$$C_{I}^{B}\,\Delta\underline{\xi}^{I} = \Delta\underline{\xi}^{B} = \Delta\underline{\Xi}^{B} + \Delta\underline{\psi}_{IB}^{B}\times\underline{\xi}^{B} \tag{A-7}$$

Finally, since all vectors in (A-7) are now defined in *B* frame coordinates, we can dispense with the superscript notation to obtain the simplified form

$$\Delta\underline{\xi} = \Delta\underline{\Xi} + \Delta\underline{\psi}\times\underline{\xi} \tag{A-8}$$

where $\Delta\underline{\psi}$ is the angular rotation of the body relative to non-rotating coordinates, and during the $\Delta\underline{\psi}$ rotation, $\Delta\underline{\Xi}$ is the change in $\underline{\xi}$ observed in rotating coordinates, and $\Delta\underline{\xi}$ is the change in $\underline{\xi}$ observed in a non-rotating coordinate frame that is instantaneously aligned with the rotating frame.

For infinitesimally small Δ increments (*d*), finite rotation Eq. (A-6) reduces to the differential form

$$d\underline{\xi}^I = C_B^I\left(d\underline{\Xi}^B + d\underline{\psi}_{IB}^B \times \underline{\xi}^B\right) \tag{A-9}$$

Similarly, for infinitesimally small Δ increments, (A-8) reduces to its simplified differential equivalent:

$$d\underline{\xi} = d\underline{\Xi} + d\underline{\psi} \times \underline{\xi} \tag{A-10}$$

where it is understood that all vectors in (A-10) are projections on the *B* (or another common) coordinate frame:

APPENDIX B
ROTATIONAL DYNAMICS OF MASS GROUPS

The angular momentum $\underline{h}_{i/0}^I$ of a mass m_i at point *i* relative to an arbitrary point 0 is traditionally defined in non-rotating inertial *I* frame coordinates [6, pp. 132] as

$$\underline{h}_{i/0}^I \equiv m_i\, \underline{r}_{i/0}^I \times \frac{d\,\underline{r}_{i/0}^I}{dt} \tag{B-1}$$

where $\underline{r}_{i/0}^I$ is the distance vector from point *0* to point *i* in *I* frame coordinates (superscript), and $d\,\underline{r}_{i/0}^I$ is the infinitesimal change in $\underline{r}_{i/0}^I$ during the infinitesimal time interval *dt*. The summation of (B-1) over a group of mass points yields the *I* frame angular momentum $\underline{h}_0^I$ of the group relative to point *0*:

$$\underline{h}_0^I = \sum_i \underline{h}_{i/0}^I = \sum_i \left(m_i\, \underline{r}_{i/0}^I \times \frac{d\,\underline{r}_{i/0}^I}{dt} \right) \tag{B-2}$$

The rate of change of $\underline{h}_0^I$ is the derivative with time of (B-2):

$$\frac{d\,\underline{h}_0^I}{dt} = \sum_i m_i \left[\frac{d\,\underline{r}_{i/0}^I}{dt} \times \frac{d\,\underline{r}_{i/0}^I}{dt} + \underline{r}_{i/0}^I \times \frac{d^2\,\underline{r}_{i/0}^I}{dt} \right] = \sum_i m_i\, \underline{r}_{i/0}^I \times \frac{d^2\,\underline{r}_{i/0}^I}{dt} \tag{B-3}$$

Ref. [5, Eqs. (3) & (6)] shows that

$$\frac{d^2\,\underline{r}_{i/0}^I}{dt} = \underline{a}_{SF\,i}^I - \underline{a}_{SF\,0}^I + \underline{g}_i^I - \underline{g}_0^I \tag{B-4}$$

where $\underline{a}^I_{SF\,i}$, $\underline{a}^I_{SF\,0}$ are the specific force accelerations at points *0* and *i*, and $\underline{g}^I_i$, $\underline{g}^I_0$ are the gravitational accelerations at these points. Because points *i* and *0* are sufficiently close, $\underline{g}^I_i \approx \underline{g}^I_0$. Then with (B-4), (B-3) becomes

$$\frac{d\,\underline{h}^I_0}{dt} = \sum_i m_i\,\underline{r}^I_{i/0} \times \left(\underline{a}^I_{SF\,i} - \underline{a}^I_{SF\,0}\right) \tag{B-5}$$

Applying Newton's second law of motion to (B-5) equates $m_i\,\underline{a}^I_{SF\,i}$ to the force $\underline{F}_i$ at point *i* that produced it, hence:

$$\frac{d\,\underline{h}^I_0}{dt} = \sum_i \underline{r}^I_{i/0} \times \underline{F}^I_i - \left(\sum_i m_i\,\underline{r}^I_{i/0}\right) \times \underline{a}^I_{SF\,0} \tag{B-6}$$

The center of mass *cm* of the mass group is analytically defined to be at distance vector $\underline{r}^I_{cm/0}$ from point *0* such that it's product with the total group mass *M* equals $\sum_i m_i\,\underline{r}^I_{i/0}$:

$$M \equiv \sum_i m_i \qquad M\,\underline{r}^I_{cm/0} = \sum_i m_i\,\underline{r}^I_{i/0} \tag{B-7}$$

With (B-7), (B-6) becomes

$$\frac{d\,\underline{h}^I_0}{dt} = \sum_i \underline{r}^I_{i/0} \times \underline{F}^I_i - M\,\underline{r}^I_{cm/0} \times \underline{a}^I_{SF\,0} \tag{B-8}$$

By selecting arbitrary point *0* as the center-of-mass (point *cm*) for the group, $\underline{r}^I_{cm/0}$ is zero, and (B-8) reduces to

$$\frac{d\,\underline{h}^I_{cm}}{dt} = \sum_i \underline{r}^I_{i/cm} \times \underline{F}^I_i \tag{B-9}$$

where $\underline{h}^I_{cm}$ is the angular momentum of the mass group around the group center of mass. By Newton's third law, the interactive forces between adjacent mass points at any point *i* are equal and opposite. Hence, the internal/interactive moment/force terms cancel at each *i* point and (B-9) further simplifies to the more familiar form [6, pp. 132]:

$$\frac{d\,\underline{h}^I_{cm}}{dt} = \sum_i \underline{r}^I_{i/cm} \times \underline{F}^I_{External\,i} = \sum_i \underline{T}^I_{i/cm} \tag{B-10}$$

where $\underline{F}^I_{External_i}$ is the external force applied to the group at point *i*, and $\underline{T}^I_{i/cm}$ is the associated torque around the center of mass, i.e., $\underline{T}^I_{i/cm} \equiv \underline{r}^I_{i/cm} \times \underline{F}^I_{External_i}$.

REFERENCES

[1] Savage, P. G., "Strapdown Sensors", Article 2, *NATO AGARD Lecture Series 95, Strap-Down Inertial Systems*, June 1978.

[2] Savage, P.G., "Analytical Description of Optical Gyros", WBN-14024, April 3, 2019 (Updated November 6, 2022 and February 28, 2024), free access available at www.strapdowassociates.com.

[3] Einstein, A., *Relativity, The Special and the General Theory*, 1961, The Estate of Albert Einstein.

[4] Savage, P. G., *Strapdown Analytics, Edition II*, Strapdown Associates, Inc., 2007, available for purchase at www.strapdownassociates.com.

[5] Savage, P.G., "Redefining Gravity And Newtonian Natural Motion", SAI-WBN-14002, May 21, 2014 (Updated September 28, 2022), free access available at www.strapdowassociates.com.

[6] Halfman, R. L., *Dynamics: Particles, Rigid Bodies, and Systems, Volume I*, Addison-Wesley, Reading Mass., Palo Alto, London, 1962.